SUPPLEMENTAL TABLES AND FIGURES

Supplemental Table 1. Pathology of 19.5-month old *NHERF1* deficient mice.

Pathology	Males		Females	
	WT (n=7)	**KO** (n=9)	**WT** (n=10)	**KO** (n=7)
Malignancies[1]	14%	22%	50%	43%
Lymphoid hyperplasia[2]	86%	100%	40%	57%
Nephropaties[2,3]	14%	44%	10%	71%
Lymphocytic dacryo/sialoadenitis[2]	0%	33%	10%	43%

WT, NHERF1$^{+/+}$; KO, NHERF1$^{-/-}$

[1]Malignancies comprise lymphoma and histiocytic sarcoma, which are relatively common neoplasms in aged mice. One NHERF1$^{-/-}$ male developed a malignant submucosal stromal tumor of the urinary bladder.

[2]These lesions may be associated with aging.

[3]Nephropaties comprise glomerulonephritis and lymphocytic tubulointerstitial nephritis.

Supplemental Table 2. % difference by which intestinal tumor load is increased in *NHERF1* knockout versus *NHERF1* wild-type mice.

Tumors		All	Males	Females
Tumor density	Total*	+45	+18	+67
	Small intestine	+45	+24	+60
Adenoma	Total	+105	+45	+177
	1-1.5 mm	+106	+63	+145
	1.5-2 mm	+57	-3	+167
	2-2.5 mm	+67	+7	+167
	>2.5 mm	+633	+148	#

* The counts for colon polyps are low (see Fig. 3B) and therefore they have been integrated in the % difference for the total number.

% difference cannot be expressed for this category, as the >2.5 mm adenoma tumor count is 2.33 in average for knockout females but 0 in wild-type females.

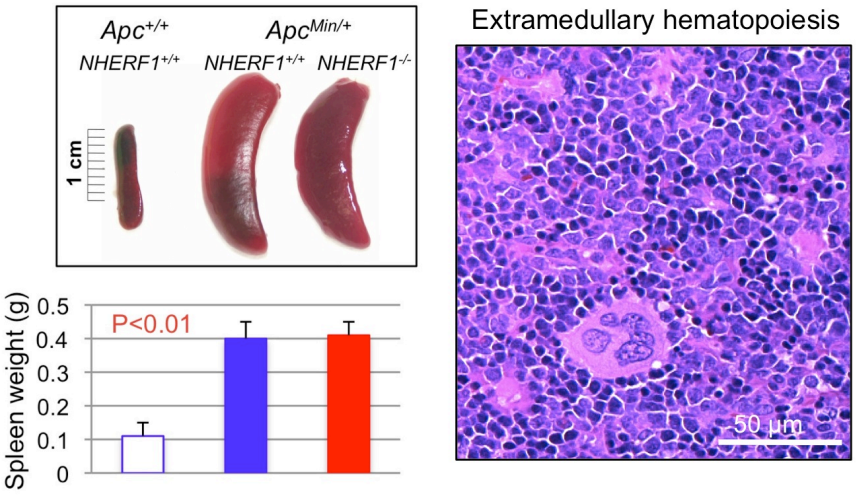

Figure S1. Massively enlarged spleens in both control *Apc*$^{Min/+}$*NHERF1*$^{+/+}$ and *Apc*$^{Min/+}$*NHERF1*$^{-/-}$ double mutant mice. The graph shows the spleen weight of *Apc*$^{Min/+}$*NHERF1*$^{+/+}$ (n=8) and *Apc*$^{Min/+}$*NHERF1*$^{-/-}$ (n=6) mice compared to wild-type littermates (n=2), as means±SEM. H&E histology shows that spleen enlargement is due to extramedullary hematopoiesis.

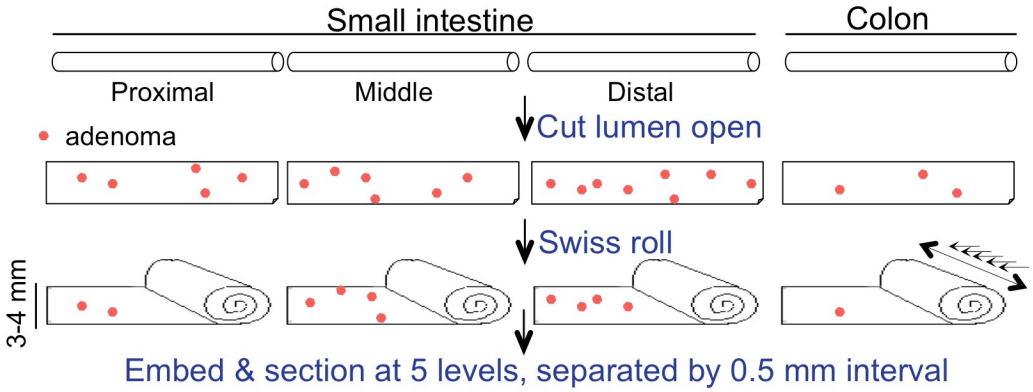

Figure S2. Technique of Swiss-rolling (see also Material and Methods). The small intestine and colon are dissected from mice and gently flushed with cold PBS. The small intestine is sectioned into three equal segments: proximal, middle and distal, roughly corresponding to duodenum, jejunum and ileum. These fragments and the colon are cut open, rolled onto themselves and embedded on edge.

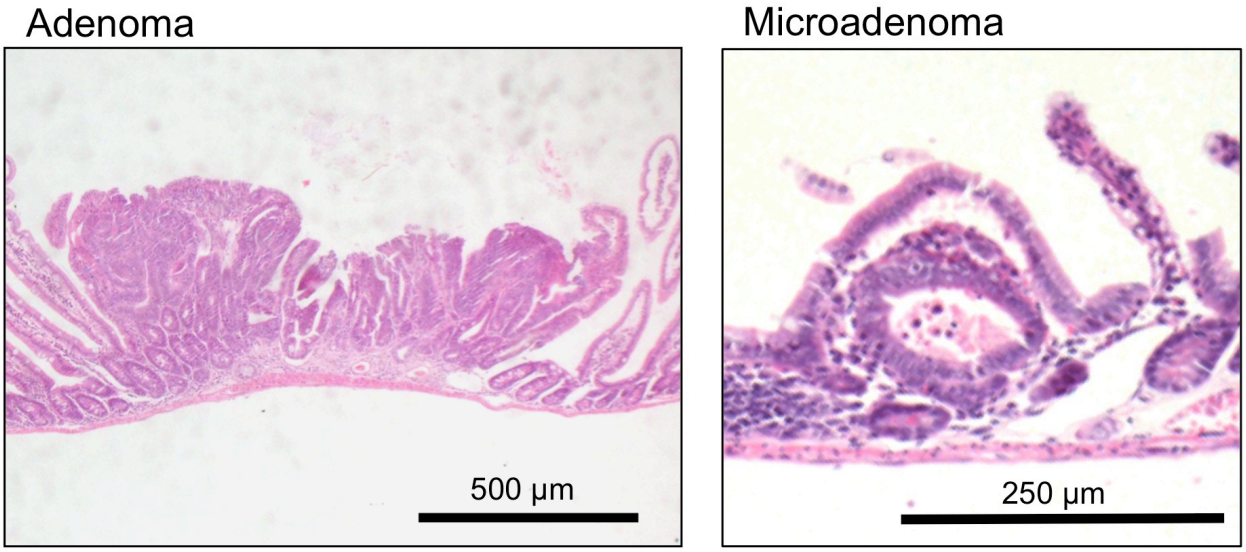

Figure S3. Neoplastic lesion count. Adenomas and microadenomas (diameter < 1 mm) were counted. The left panel shows a typical broad-based adenoma. The right panel shows the smallest lesion in the microadenoma range: a single gland microadenoma or dysplastic aberrant crypt focus. Both are from the small intestine middle segment of a16-week-old *Apc*$^{Min/+}$*NHERF1*$^{+/+}$ male mouse.

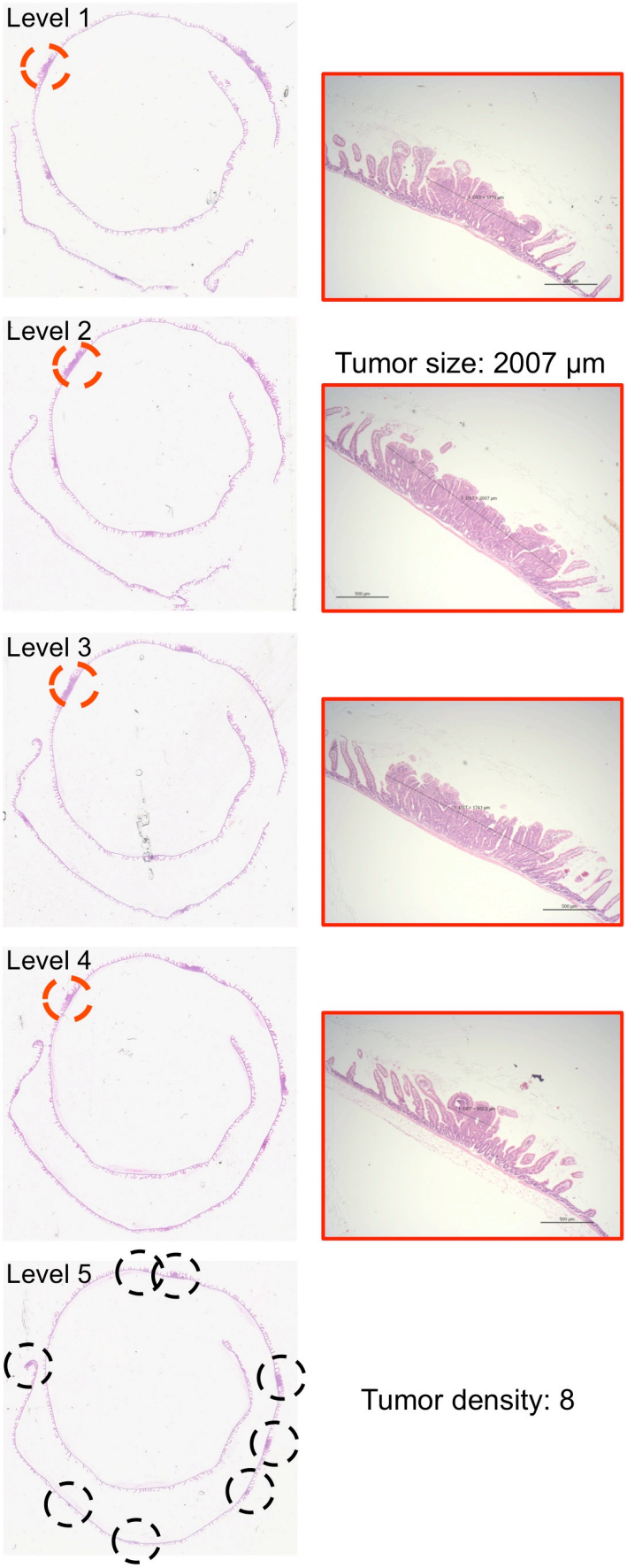

Figure S4. Scoring adenoma size and tumor density. H&E of small intestine middle segment Swiss-roll from an *Apc*$^{Min/+}$*NHERF1*$^{+/+}$ female mouse shows the five levels analyzed. The adenomas and microadenomas were counted on each level and the highest number of tumors on one level was scored as tumor density. For the illustrated case, levels 1 and 5 had the highest number of tumors, 8 each, which represents the tumor density for this segment. All the lesions with a diameter ≥ 1 mmm (adenomas) were measured and followed through the five levels. The highest dimension corresponding to a given tumor was recorded as the size of that tumor. In the illustrated case, the tumor encircled with a red line appears on four levels, as shown in the insets. The highest dimension was seen on level 2 and recorded as the size of this adenoma. Note that this scoring system takes in account the total number of adenomas growing in the intestine, whereas the tumor density refers to the highest local density of tumors for a given intestinal segment. Due to random sectioning that could miss the equator of the lesions, the scored adenoma size is equal or smaller than the real adenoma size.

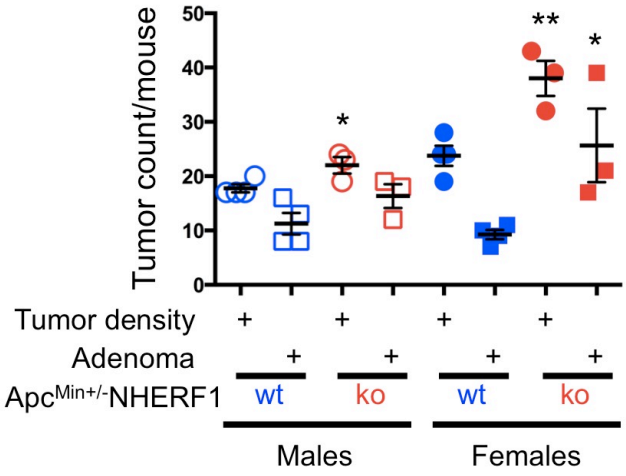

Figure S5. Increased tumor burden in *Apc*$^{Min/+}$*NHERF1*$^{-/-}$ mice. The tumor density and number of adenomas in the small intestine per mouse are shown side by side in male and female *Apc*$^{Min/+}$*NHERF1*$^{+/+}$ and *Apc*$^{Min/+}$*NHERF1*$^{-/-}$ mice. Data are plotted as mean±SEM from individual values representing the counts from each individual mouse. Statistical significant differences versus the corresponding control group are indicated: *, $p<0.05$; **, $p<0.001$. Note relatively close individual values for tumor density within the same genotype group.

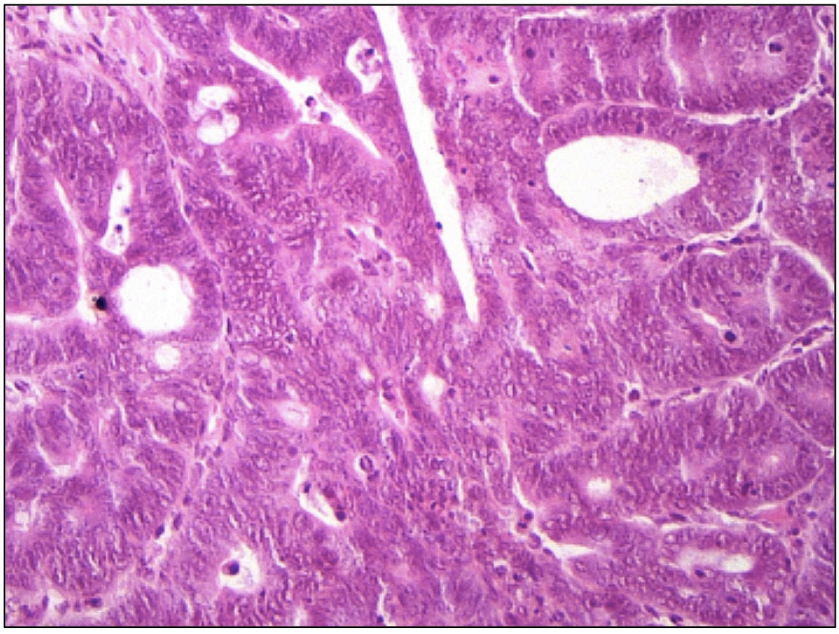

Figure S6. Histology of tubular adenoma. H&E of a colonic polyp from an *Apc*$^{Min/+}$*NHERF1*$^{-/-}$ female showing the histology of a tubular adenoma with high-grade dysplasia. Loss of normal glandular architecture, focal cribriform pattern, hyperchromatic cells with multilayered nuclei and high nuclear-cytoplasmic ratio are attributes of high-grade dysplasia.

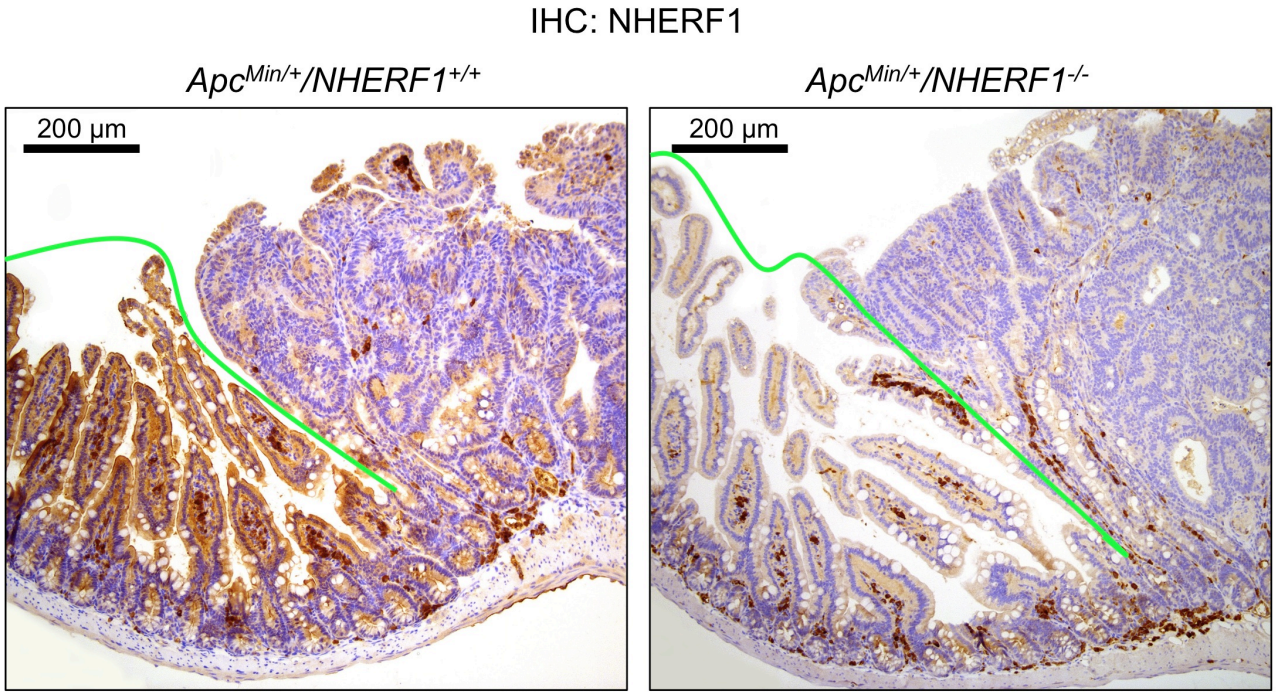

Figure S7. Loss of NHERF1 expression in adenoma. IHC with NHERF1 antibody (Thermo/Fisher) shows apical and cytoplasmic expression in normal *Apc*$^{Min/+}$*NHERF1*$^{+/+}$ mucosa and loss of expression in adenoma. A green line separates the normal and transformed components. The images were acquired from the distal fragment of the small intestine. For this IHC, the secondary antibody is a mouse antibody that labels Fc receptor-expressing cells in both NHERF1 wild-type and knockout tissues.

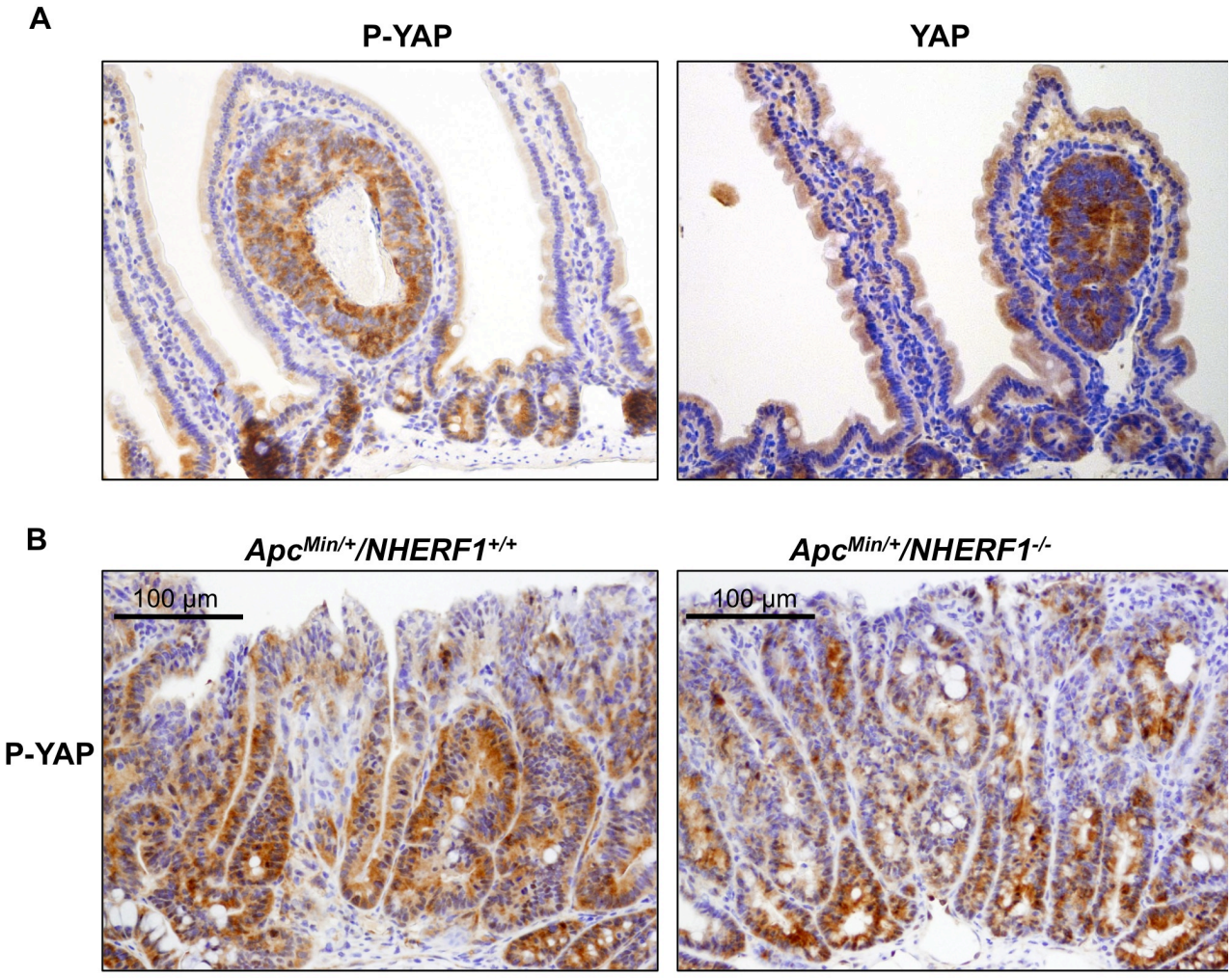

Figure S8. YAP and phopshorylated YAP (P-YAP) expression in normal and neoplastic tissue from *Apc*$^{Min/+}$*NHERF1*$^{+/+}$ and *Apc*$^{Min/+}$*NHERF1*$^{-/-}$ mice. **A.** IHC with P-YAP and YAP antibodies shows cytoplasmic expression limited to crypts in the normal mucosa, and comparable expression levels in crypts and aberrant crypt foci. **B.** IHC analysis with P-YAP antibody of polyps of comparable size from distal small intestine shows overall lower expression levels in *Apc*$^{Min/+}$*NHERF1*$^{-/-}$ mice relatively to *Apc*$^{Min/+}$*NHERF1*$^{+/+}$ mice.